Available online at www.sciencedirect.com

ScienceDirect

Procedia Structural Integrity 8 (2018) 379–389

Structural Integrity Procedia

www.elsevier.com/locate/procedia

AIAS 2017 International Conference on Stress Analysis, AIAS 2017, 6–9 September 2017, Pisa, Italy

Shape optimization using structural adjoint and RBF mesh morphing

C. Groth[a], A. Chiappa[a], M.E. Biancolini[a,*]

[a]*Department of Enterprise Engineering - University of Rome Tor Vergata, Via del Politecnico, 1, 00133, Rome, Italy*

Abstract

Adjoint solvers are acquiring nowadays a growing importance in shape optimization especially when dealing with fluid dynamic applications; their use for structural optimization is however still limited. In this work an optimization workflow based on the synergic use of a structural continuum-discrete adjoint variable solver and the commercial morpher RBF Morph™ is presented. Shape sensitivity information with respect to the objective function is exported as deformation maps on the interested geometry and transferred to the morpher that, after a proper filtering and setup, allows to update automatically the numerical grid. By employing a gradient based logic it is finally possible to achieve an evolutionary optimization. The proposed method effectiveness is shown with two examples: a cantilever beam and a structural bracket.

Peer-review under responsibility of the Scientific Committee of AIAS 2017 International Conference on Stress Analysis

Keywords: Adjoint; Sensitivity; FEM; Shape optimization; RBF

1. Introduction

During the years numerical analysis assumed a growing importance in the engineering practice, obtaining a crucial and irreplaceable role in the design phase. Complex systems and physics can be studied in a short amount of time, foreseeing their behavior with great accuracy. Having the ability to study faithfully a system - being it mechanic, fluid dynamic or dominated by other physics - means also to be able to evaluate the influence of its boundary conditions by examining their effect before and after their variation. The main problem of understanding how to apply these variations in the most efficient way however remains, being relevant and difficult especially when dealing with a shape change.

In engineering applications the most employed methods are zero order ones. While carrying a set of useful features, such as their ability to reach a global optimum and the relatively easy implementation, their cost can be unbearable when dealing with an high number of objective functions and parameters. This property, at the price of finding a local optimum, is covered by optimization methods based on the gradient, using in an iterative and evolutionary fashion the system sensitivities with respect to a parameter; these information, comparable with the gradient of the response

* Corresponding author. Tel.: +39 0672597124.
E-mail address: biancolini@ing.uniroma2.it

Peer-review under responsibility of the Scientific Committee of AIAS 2017 International Conference on Stress Analysis
10.1016/j.prostr.2017.12.038

surface, can be obtained by employing simple methods such as finite differences or complex differentiation but their cost remains hardly affordable when an high number of parameters is present, requiring at least an evaluation for parameter. When dealing with 3D shape optimization each node of the numerical grid, that for industrial cases can reach hundreds of millions of cells, can be seen as a parameter with three degrees of freedom, making impossible the use of these techniques for practical sensitivity calculation.

These problems however can be tackled by employing adjoint methods that allow to achieve, with a single evaluation, the sensitivity of an objective function with respect to a given number of parameters. It is then possible to obtain the sensitivity of the performance measure with respect to the displacement, in the three directions, of each mesh node, achieving the influence of a given shape parameterization (Papoutsis-Kiachagias et al. (2016), Papoutsis-Kiachagias et al. (2015)) or obtaining new ones (Groth (2015)).

In this paper an automatic gradient based optimization workflow is presented for structural applications. A new continuous-discrete adjoint solver was implemented and embedded in ANSYS ® Mechanical™, obtaining sensitivity maps with respect to the shape variations of the surfaces interested by the optimization. These information are conveniently filtered and transferred, with a special setup conceived in order to respect functional and packaging constraints, to the commercial morpher based on Radial Basis Functions (RBF) RBF Morph ACT Extension. By employing a gradient based optimization logic this workflow can be automated obtaining the optimum in an evolutive fashion.

2. Adjoint

2.1. Sensitivity for structural applications

A large number of methods exists to obtain the sensitivity value of a system with respect to a parameter; simple methods such as finite differences (Thomée (2001), Lewy et al. (1928)) or complex-step differentiation (Lyness and Moler (1967), Squire and Trapp (1998)) can evaluate approximately its influence by using only outputs and inputs, making the whole system and its modelization a black box. Their approximate nature, however, makes results highly susceptible to numerical errors and so their use limited and not generic. Given also the need of evaluating the system at least before and after the parameter change for each objective function, these methods result to be inefficient and unbearable when dealing with an high number of parameters.

To tackle these problems, similarly to what done for fluid dynamic applications (Nadarajah and Jameson (2001), Newman and Taylor (1999)), it is possible to work directly on the physics that describe the problem by differentiating the discretized equations of finite elements (Brockman and Lung (1988), Yatheendhar and Belegundu (1993), Francavilla et al. (1975)) or by deriving the equations prior to their differentiation (Dems and Mroz (1983), Dems and Haftka (1988)). In the first case the method employed is called discrete, in the latter continuous. Taking into account, for the sake of simplicity, the discrete method, be the objective function used to optimize the structural system in the form:

$$\Psi = f(\mathbf{X}(u), u) \tag{1}$$

that depends on the structural displacements X and is directly and indirectly influenced by the parameter u. Its variation, in function of the given parameter, can be calculated as:

$$\frac{d\Psi}{du} = \frac{\partial\Psi}{\partial u} + \frac{\partial\Psi}{\partial\mathbf{X}}\frac{\partial\mathbf{X}}{\partial u} \tag{2}$$

Where $\frac{\partial\Psi}{\partial u}$ and $\frac{\partial\Psi}{\partial\mathbf{X}}$ are terms generally easy to be calculated being explicit and knowing the analytical expression of Ψ. The term $\frac{\partial\mathbf{X}}{\partial u}$ by the other hand shows an implicit dependence and it is more difficult to be calculated. To obtain this term two methods can be employed, namely the direct or the adjoint method.

For a static problem it is indeed:

$$\mathbf{KX} = \mathbf{F} \tag{3}$$

For which the variation with respect to a given parameter u is:

$$\mathbf{K}\frac{\partial \mathbf{X}}{\partial u} + \mathbf{X}\frac{\partial \mathbf{K}}{\partial u} = \frac{\partial \mathbf{F}}{\partial u} \tag{4}$$

that allows to obtain the variation of the structural behavior when changing u noticing that, moving the second member to the left:

$$\mathbf{K}\frac{\partial \mathbf{X}}{\partial u} = \frac{\partial \mathbf{F}}{\partial u} - \mathbf{X}\frac{\partial \mathbf{K}}{\partial u}. \tag{5}$$

similarly to (3) the last one is a structure with stiffness $\mathbf{K}$ but this time subject to a fictitious load equal to $\frac{\partial \mathbf{F}}{\partial u} - \mathbf{X}\frac{\partial \mathbf{K}}{\partial u}$. As a result of the analysis it will be obtained the displacement field $\frac{\partial \mathbf{X}}{\partial u}$ that can be employed to solve equation (2), obtaining:

$$\frac{d\Psi}{du} = \frac{\partial \Psi}{\partial u} + \frac{\partial \Psi}{\partial \mathbf{X}}\mathbf{K}^{-1}\left(\frac{\partial \mathbf{F}}{\partial u} - \mathbf{X}\frac{\partial \mathbf{K}}{\partial u}\right) \tag{6}$$

that is the direct method for structural sensitivity calculation. It should be noticed that for each parameter the (5) should be calculated again, calculation not required instead when is the performance measure Ψ in equation (6) to be changed.

The adjoint method differs from the direct one by using a term, called adjoint variable, that can be seen as a Lagrange multiplier (Belegundu (1985)) of the constraint (3) in the Lagrangian built together with (1). The adjoint variable, multiplied for the stiffness matrix, allows to obtain the adjoint equation:

$$\mathbf{K}\lambda = \frac{\partial \Psi^{\mathrm{T}}}{\partial \mathbf{X}} \tag{7}$$

That is the same structure of (3) with a fictitious load equal to $\frac{\partial \Psi}{\partial \mathbf{X}}^{\mathrm{T}}$. Obtained displacements are then employed in (6) obtaining the following equation:

$$\frac{d\Psi}{du} = \frac{\partial \Psi}{\partial u} + \lambda^{\mathrm{T}}\left(\frac{\partial \mathbf{F}}{\partial u} - \mathbf{X}\frac{\partial \mathbf{K}}{\partial u}\right). \tag{8}$$

By using the adjoint method, differently to what seen with the direct one, it is possible to perform only one added calculation independently of the number of parameters. The adjoint calculation (7) doesn't depend, as a matter of fact, from the parameter u but from the performance measure Ψ: a new adjoint calculation must be performed only when a new objective function must be obtained.

Direct and adjoint method are then efficient depending on the case: if m objective functions Ψ and p parameters u are present, the direct method is advisable when there are more objective functions than parameters, meaning $m \gg p$ requiring only $p + 1$ added analyses. When by the other hand more parameters of objective functions are present and then $m \ll p$ the adjoint method is preferable requiring only $m + 1$ calculations. When dealing with shape optimization there are up to three parameters per node, making the adjoint solver the best option.

2.2. Adjoint solver implementation

The new adjoint solver implemented and employed in this paper is continuous-discrete. The adjoint equations and the equations describing the system are derived from the variational formulation. The obtained continuous and numerically exact form is successively discretized by using the Galerkin method in correspondence of the numerical grid.

When dealing with a shape parameterization requiring substantial derivatives (Choi and Haug (1983)), the adjoint equation is obtained by deriving the performance measure Ψ by collecting all the terms in which there is an implicit dependence from the shape parameter. Being at equilibrium:

$$a(z, \bar{z}) = l(\bar{z}) \tag{9}$$

where $a(z, \bar{z})$ is the energy bilinear and $l(\bar{z})$ is the linear form of the work done by external loads in variational form. It can be demonstrated that, once solved the adjoint equation with the fictitious loads similarly to what done in (7), the following relation exists:

$$\Psi' = l'(\lambda) - a'(z, \lambda) + H \tag{10}$$

Where H are all the terms of easy calculation showing explicit dependence on the shape parameter. This form is particularly suitable for numerical implementation, being $a'(z, \lambda)$ and $l'(\lambda)$ peculiar and derivable for each element formulation, such as Mindlin-Reissner plates, Timoshenko beams or solid elements. Exploiting this feature the solver was developed modularly, obtaining the sensitivities by using only the baseline and the adjoint calculation. Taking advantage on ACT technology the solver was integrated in ANSYS Mechanical, allowing to setup the structural calculation and reading directly the results of baseline and adjoint analyses. Being the energy bilinear $a'(z, \lambda)$ the same for baseline or fictitious loads (as seen for the discrete form in (7)), the same structure was employed using a multi-step calculation in order to speed up the evaluation.

The sensitivity value of the objective function with respect to the displacement in the three cartesian directions is exported as a deformation map, obtaining an accurate hint on how to remodel the geometry node by node.

Mesh movement is obtained by using the commercial morpher RBF Morph, enabling an accurate local node by node control using Radial Basis Functions (RBF).

3. Morphing

3.1. RBF interpolation

RBF are mathematical functions able to interpolate, on a distance basis, scalar information known only at discrete points (source points). The quality and the behavior of the interpolation depends both from the function and from the kind of chosen basis function: RBF can be indeed classified depending on the kind of support they guarantee (local or global), meaning the domain in which the function is not zero valued (de Boer et al. (2007)). Some of the most common functions are shown in table 1. RBF can be defined in an n dimension space and are function of the distance which, in the case of morphing, can be assumed as the euclidean norm of the distance between two points in the space.

Table 1. Common RBF with global and local support.

Compactly supported RBF	Abbreviation	$\phi(\zeta)$
Wendland C^0	$C0$	$(1-\epsilon\zeta)^2$
Wendland C^2	$C2$	$(1-\epsilon\zeta)^4(4\epsilon\zeta+1)$
Wendland C^4	C4	$(1-\epsilon\zeta)^6(\frac{35}{3}\epsilon\zeta^2+6\epsilon\zeta+1)$
Globally supported RBF	**Abbreviation**	$\phi(\zeta)$
Polyharmonic spline	PHS	r^n, n odd $r^n log(r)$, n even
Thin plate spline	TPS	$r^2 log(r)$
Multiquadric biharmonics	MQB	$\sqrt{a^2+(\epsilon r)^2}$
Inverse multiquadric biharmonics	IMQB	$\frac{1}{\sqrt{a^2+(\epsilon r)^2}}$
Quadric biharmonics	QB	$1+(\epsilon r)^2$
Inverse quadric biharmonics	IQB	$\frac{1}{1+(\epsilon r)^2}$
Gaussian biharmonics	GS	$e^{-\epsilon r^2}$

A linear system of order equal to the number of points used (Buhmann (2000)) must be solved in order to find system coefficients. Once the coefficients are found, the displacement of a given node of the mesh, being it inside (interpolation) or outside the domain (extrapolation), can be calculated as the superimposition of the radial contribution of each source point. It is then possible to define at known points the displacement in the space and to retrieve the value at mesh nodes, obtaining a mesh deformation that leaves unaltered grid topology (Beckert and Wendland (2001)).

The interpolation function is composed by the basis ϕ and by the polynomial term h with a degree that depends on the kind of the chosen basis. This latter contribution, in particular, is added to assure uniqueness of the problem and polynomial precision, allowing to recover exactly rigid body motions. If N is the total number of source points it follows:

$$s(\mathbf{x}) = \sum_{i=1}^{N} \gamma_i \phi(\|\mathbf{x} - \mathbf{x}_{k_i}\|) + h(\mathbf{x}) \tag{11}$$

An interpolation exists if coefficients and weights of the polynomial can be found such that the given value at source points can be retrieved exactly. At source points the polynomial contribution should be zero. It is then:

$$s(\mathbf{x}_{k_i}) = g_i, 1 \leq i \leq N \qquad \text{and} \qquad \sum_{i=1}^{N} \gamma_i p(\mathbf{x}_{k_i}) = 0 \tag{12}$$

for all the polynomials p of degree less or equal to polynomial h. A single interpolant exists if the basis is conditionally positive definite (Micchelli (1986)). If the degree is $m \leq 2$ (Beckert and Wendland (2001)) a linear polynomial can be used:

$$h(\mathbf{x}) = \beta_1 + \beta_2 x_1 + \beta_3 x_2 + ... + \beta_{n+1} x_n \qquad \text{in} \qquad \mathbb{R}^n \tag{13}$$

The system built to calculate coefficients and weights can be easily written in matrix form for an easy implementation:

$$\begin{bmatrix} \mathbf{M} & \mathbf{P} \\ \mathbf{P}^T & \mathbf{0} \end{bmatrix} \begin{Bmatrix} \boldsymbol{\gamma} \\ \boldsymbol{\beta} \end{Bmatrix} = \begin{Bmatrix} \mathbf{g} \\ \mathbf{0} \end{Bmatrix} \tag{14}$$

Where $\mathbf{g}$ is is the vector of known terms for each source point and $\mathbf{M}$ is the interpolation matrix with the radial distances between source points:

$$M_{ij} = \phi(\|\mathbf{x}_{k_i} - \mathbf{x}_{k_j}\|), 1 \leq i \leq N, 1 \leq j \leq N \tag{15}$$

$\mathbf{P}$ is the constraint matrix containing the coordinates of source points in the space:

$$\mathbf{P} = \begin{pmatrix} 1 & x_{k_1} & y_{k_1} & z_{k_1} \\ 1 & x_{k_2} & y_{k_2} & z_{k_2} \\ \vdots & \vdots & \vdots & \\ 1 & x_{k_N} & y_{k_N} & z_{k_N} \end{pmatrix} \tag{16}$$

Once the weights and and coefficients of the system are obtained, the displacement values can be retrieved for the three directions at a given $\mathbf{X}$ point as (Biancolini (2012)) :

$$\begin{cases} S_x(\mathbf{x}) = \sum_{i=1}^{N} \gamma_i^x \phi(\|\mathbf{x} - \mathbf{x}_{k_i}\|) + \beta_1^x + \beta_2^x x_1 + \beta_3^x x_2 + \beta_4^x x_n \\ S_y(\mathbf{x}) = \sum_{i=1}^{N} \gamma_i^y \phi(\|\mathbf{x} - \mathbf{x}_{k_i}\|) + \beta_1^y + \beta_2^y x_1 + \beta_3^y x_2 + \beta_4^y x_n \\ S_z(\mathbf{x}) = \sum_{i=1}^{N} \gamma_i^z \phi(\|\mathbf{x} - \mathbf{x}_{k_i}\|) + \beta_1^z + \beta_2^z x_1 + \beta_3^z x_2 + \beta_4^z x_n \end{cases} \tag{17}$$

3.2. RBF Morph ACT extension

The modular architecture of ANSYS Workbench allows to extend its functionalities by using an add-on logic with ACT technology. The commercial morpher RBF Morph ACT extension manages the task of mesh updating. The software is integrated in the ANSYS mechanical interface sharing with it the interaction logics such as the selection tools and named selections (Cenni et al. (2015)) and is located in the mechanical three inside the project as shown in Figure 1.

The modeling logic using RBF Morph ACT extension is hierarchical, allowing to prescribe through the use of suitable shape modifiers (translation, rotation, scaling, curve projection, surface projection, curve and surface offsets) displacements at mesh nodes obtaining complex shapes in a parametric fashion (Costa et al. (2015)).

The automatic link between adjoint solver and morpher was obtained by exploiting an RBF Morph functionality called ACT^2, which allows to have access, at low level and from other ACT extensions, to the most important features of the software. In this case the displacement of each node from the interested surfaces was given at each optimization cycle, obtaining automatically the evolutive variation of the geometry.

3.3. Optimization set-up

To obtain an automatic and evolutive variation of the geometry while maintaining the functional and packaging constraints, it was adopted a two sets strategy, defining one fixed and one moving points set. The fixed points set contains all the zero translation source points applied to surfaces or the mesh portions that must remain undeformed,

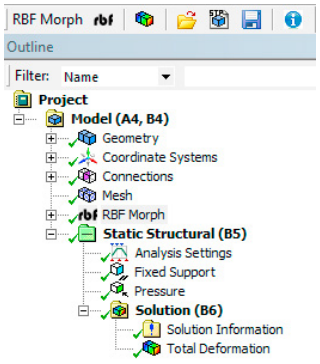

Fig. 1. RBF Morph integration in the Mechanical tree

constraining their motion. It is also possible to control volume mesh deformation, restricting the morphing action by using fixed points in the numerical grid volume. The fixed set remains unaltered during the optimization. On the other hand the moving points set is generated automatically at each optimization cycle by filtering the sensitivity map selectively, on a geometrical basis. Source points are located only where the deformation given by the adjoint solver must be applied.

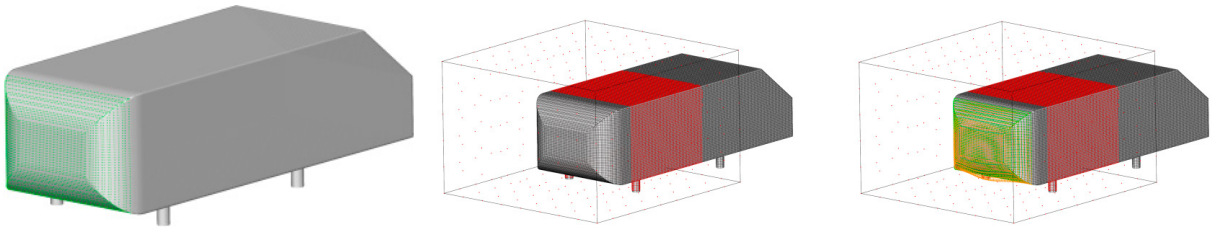

Fig. 2. From left to right: moving set, fixed set and complete set-up

The two sets are then overlapped at each optimization iteration obtaining a single RBF problem that varies automatically and evolutively without user interaction. In figure 2 an example of this approach is shown for an aerodynamic application on an Ahmed body: the moving set, filtered from the sensitivity map in order to maintain only the points of the nose and shown in green, is blended to the fixed points set shown in the center image to obtain the complete set-up. As it can be seen in the right image of figure 2 moving and fixed sets never overlap but maintain a buffer zone in order to smoothly spread deformations in the mesh, avoiding excessive distortions of the numerical grid.

4. Optimization workflow

The shape variation obtained with this strategy, partially faithful to the sensitivity map given by the adjoint solver but filtered using fixed sets, must be employed to evaluate its influence on the observable.

The recalculated value can be used to make the geometry evolve by relying on an optimization algorithm based on the gradient: as a search direction can be used the sign of the foreseen observable variation and as a step its value.

The optimization workflow employed in this paper is shown in figure 3. The tasks carried by the adjoint solver are highlighted in green and in light blue the ones that interest the RBF morpher.

At first the baseline numerical grid is used for a multistep analysis in which the two loading conditions are the working one and the one resulting from the application of the fictitious loads as shown in (7).

Results for both steps, in terms of displacements, are read by the adjoint solver and used for the sensitivity map calculation. The sensitivity values relative to the objective function chosen for the displacement are thus available along the three directions of each mesh node. These information are filtered suitably by taking them only where needed, obtaining a displacement field acting only where the shape variation can be applied. The moving set is blended

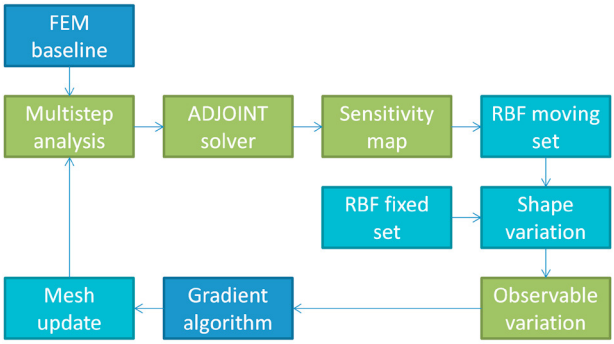

Fig. 3. RBF Morph integration in the Mechanical tree

to the fixed one, defining nodes and surfaces that cannot be moved, in order to obtain the main problem used to move the mesh.

The observable variation implicated by this shape modification, obtained using the original sensitivity map, is employed by a gradient based optimization algorithm that tunes the amplification of the shape modification and updates the numerical grid. At this point the so modified grid can be fed again to a new optimization step until a specified convergence criteria is met or when a maximum number of iterations is reached.

5. Applications

To demonstrate the workflow presented in this paper two applications are here shown: a structural bracket and a cantilever beam.

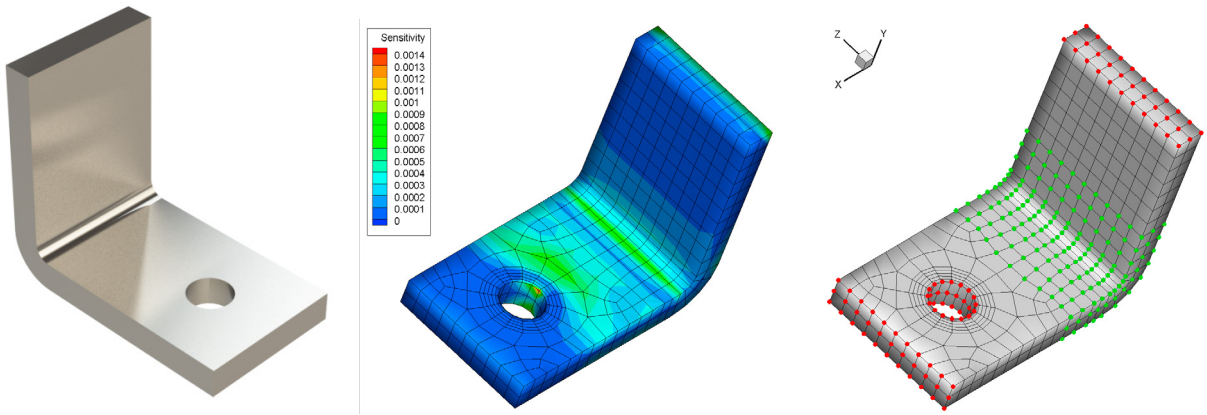

Fig. 4. Bracket baseline geometry, Sensitivity map of the free end maximum displacement with respect to nodal displacements and shape modification setup with moving set (green points) and fixed set (red points)

In figure 4 the baseline geometry of the bracket interested by the optimization is shown, built in structural steel with Young modulus of 200 GPa and 0.3 Poisson. Boundary conditions are the fixed bolt surface and a load of 5000 N along the x axis applied at the free edge.

The optimization goal is to reduce the displacement at the free end maintaining undeformed the areas near the hole and near the loaded surface. By using the information given by the adjoint solution it is possible to achieve this result by adding material in the most efficient way.

In figure 4, center, the sensitivity map of the free end displacement with respect to shape change obtained using the adjoint solver is shown. Not all the suggested displacements will be however taken into account, being filtered using

the setup illustrated in figure 4 on the right: only the nodal displacements in correspondence with green dots will be applied to each cycle.

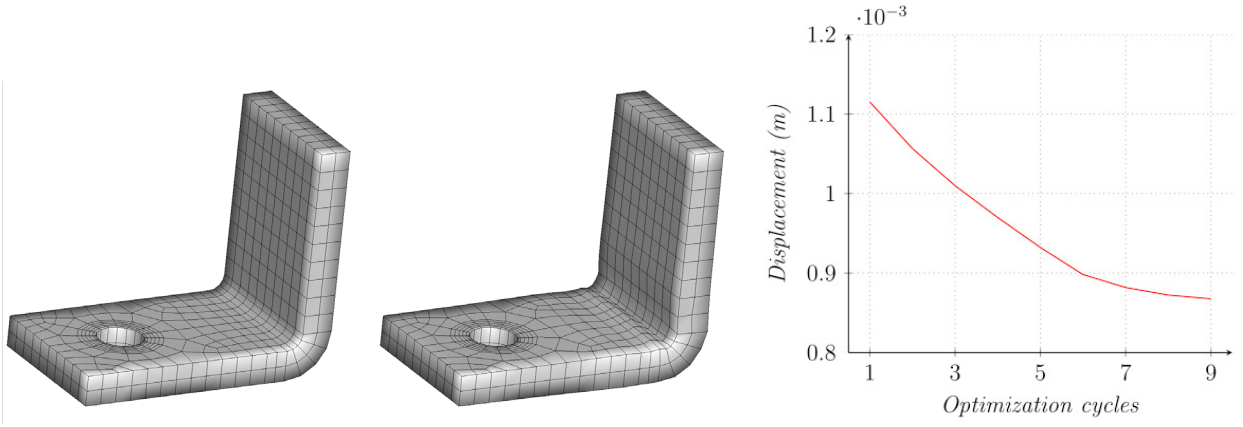

Fig. 5. Baseline geometry, optimized bracket and observable variation during optimization

The optimization, controlled by a deepest descent algorithm, was carried by tuning the optimization step in order to assure a maximum displacement of 1 mm. After 9 optimization cycles the obtained displacement reduction at the free end was 22% with respect to the baseline case. Baseline and optimized numerical grids are shown in figure 5. Constraint applied using the fixed set are correctly maintained.

In figure 5 is shown the bracket optimization history.

To obtain the same displacement reduction by employing as a shape parameter a constant variation of thickness, the required mass increase would be of 9% while, using the proposed approach, the added mass is 6% being it applied in the most influent areas.

The second example shown has, as an objective, the reduction of displacement of a simple cantilever beam.

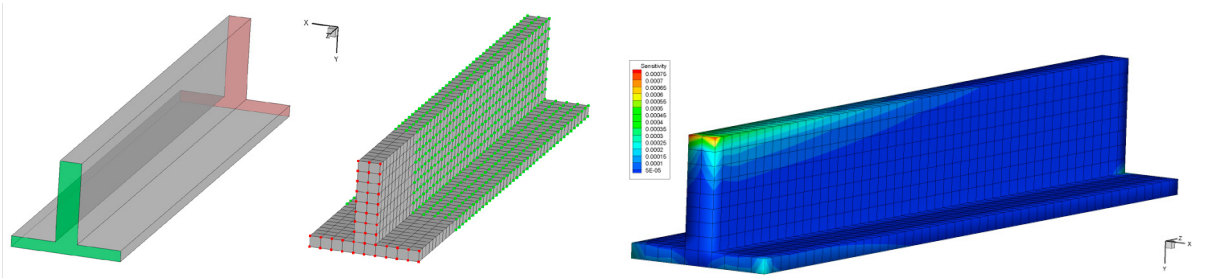

Fig. 6. Left: baseline geometry and optimization setup. Right: sensitivity map

The geometry, shown in figure 6, was modeled using a structural steel with a 200 GPa Young modulus and Poisson coefficient of 0.3 and is loaded on the green surface along the y axis with 10000N while maintaining fixed the red surface. The morphing setup was conceived in order to maintain undeformed the loaded area and by deforming the remaining ones. The sensitivity map of the free end displacement with respect to nodal deformations is shown in the right image of figure 6.

In figure 7 is shown the baseline grid and the optimized one after 22 optimization cycles. The obtained geometry was automatically modified by adding mass on the area near the constraint by following the suggestions given by the adjoint solver. The observable reduction, as shown in figure 7 to the left, is equal to 25%.

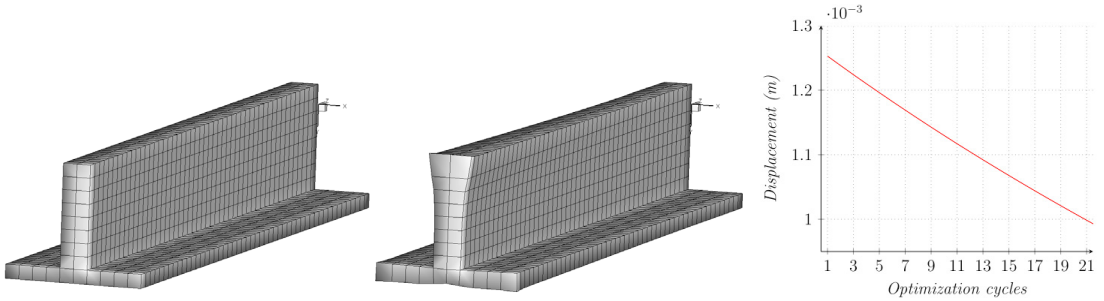

Fig. 7. Left: baseline and optimized numerical grids. Right: optimization history

6. Conclusions

The adjoint optimization method, well established for fluid dynamics applications, is here applied to structural problems. Strengths of this method are its computational and optimization efficiency, being able to obtain the required observable variation by adding or removing the smallest amount of material and requiring only one added calculation per cycle. In this context RBF are the perfect mathematical tool to apply the shape variations suggested by the adjoint sensitivities on a nodewise basis. In order to respect the packaging and functional constraints, the displacement field is suitably filtered at each optimization cycle and superimposed with a fixed setup, obtaining a new RBF problem.

Two practical applications showcase the proposed method effectiveness: a structural bracket and a cantilever beam are reshaped in order to reduce maximum displacement under a given load. Results show how the adjoint operates, locating the areas in which the addition (or removal) of material has the maximum effect on the chosen observable. Future developments foresee the introduction of more observables such as the maximum stress, and the optimization of the numerical implementation in order to make this method feasible also for complex industrial cases.

References

Beckert, A., Wendland, H., 2001. Multivariate interpolation for fluid-structure-interaction problems using radial basis functions. Aerospace Science and Technology 5, 125–134. doi:10.1016/S1270-9638(00)01087-7.

Belegundu, A.D., 1985. Lagrangian Approach to Design Sensitivity Analysis. Journal of Engineering Mechanics 111, 680–695. URL: http://ascelibrary.org/doi/10.1061/%28ASCE%290733-9399%281985%29111%3A5%28680%29, doi:10.1061/(ASCE)0733-9399(1985)111:5(680).

Biancolini, M.E., 2012. Mesh Morphing and Smoothing by Means of Radial Basis Functions (RBF), in: Handbook of Research on Computational Science and Engineering. IGI Global. volume I, pp. 347–380. doi:10.4018/978-1-61350-116-0.ch015.

de Boer, A., van der Schoot, M.S., Bijl, H., 2007. Mesh deformation based on radial basis function interpolation. Computers and Structures 85, 784–795. doi:10.1016/j.compstruc.2007.01.013.

Brockman, R.A., Lung, F.Y., 1988. Sensitivity Analysis with Plate and Shell Finite Elements. International Journal for Numerical Methods in Engineering 26, 1129–1143.

Buhmann, M.D., 2000. Radial basis functions. Acta Numerica 2000 9, S0962492900000015. doi:10.1017/S0962492900000015.

Cenni, R., Groth, C., Biancolini, M., 2015. Structural optimisation using advanced radial basis functions mesh morphing, in: AIAS 44th National Congress, AIAS 2015 - 503, 2-5 September, Messina, Messina, Italy.

Choi, K.K., Haug, E.J., 1983. Shape Design Sensitivity Analysis of Elastic Structures Shape Design Sensitivity Analysis. Journal of Structural Mechanics 11, 231–269. doi:10.1080/03601218308907443.

Costa, E., Groth, C., Biancolini, M.E., Giorgetti, F., Chiappa, A., 2015. Structural optimization of an automotive wheel rim through an RBF mesh morphing technique, in: International CAE Conference.

Dems, K., Haftka, R.T., 1988. Two Approaches to Sensitivity Analysis for Shape Variation of Structures. Mechanics of Structures and Machines 16, 501–522. URL: http://www.tandfonline.com/doi/abs/10.1080/08905458808960274, doi:10.1080/08905458808960274.

Dems, K., Mroz, Z., 1983. Variational approach by means of adjoint systems to structural optimization and sensitivity analysis-I. Variation of material parameters within fixed domain. International Journal of Solids and Structures 19, 677–692. doi:10.1016/0020-7683(83)90064-1.

Francavilla, A., Ramakrishnan, C.V., Zienkiewicz, O.C., 1975. Optimization of shape to minimize stress concentration. The Journal of Strain Analysis for Engineering Design 10, 63–70. doi:10.1243/03093247V102063.

Groth, C., 2015. Adjoint-based shape optimization workflows using RBF. Ph.d thesis. University of Rome Tor Vergata. doi:10.13140/RG.2.2.33913.06245.

Lewy, H., Friedrichs, K., Courant, R., 1928. Über die partiellen Differenzengleichungen der Mathematischen Physik. Mathematische Annalen 100, 32–74.

Lyness, J.N., Moler, C.B., 1967. Numerical Differentiation of Analytic Functions. SIAM Journal on Numerical Analysis 4, 202–210. doi:10.1137/0704019.

Micchelli, C.A., 1986. Interpolation of scattered data: Distance matrices and conditionally positive definite functions. Constructive Approximation 2, 11–22. doi:10.1007/BF01893414.

Nadarajah, S.K., Jameson, A., 2001. Studies of the continuous and discrete adjoint approaches to viscous automatic aerodynamic shape optimization, in: 15th AIAA Computational Fluid Dynamics Conference, American Institute of Aeronautics and Astronautics, Reston, Virigina. doi:10.2514/6.2001-2530.

Newman, J., Taylor, A.C., 1999. Overview of sensitivity analysis and shape optimization for complex aerodynamic configurations. Journal of Aircraft 36. doi:arc.aiaa.org/doi/pdf/10.2514/2.2416.

Papoutsis-Kiachagias, E., Andrejasic, M., Porziani, S., Groth, C., Erzen, D., Biancolini, M., Costa, E., Giannakoglou, K., 2016. Combining an RBF-based morpher with continuous adjoint for low-speed aeronautical optimization applications, in: ECCOMAS Congress 2016 - Proceedings of the 7th European Congress on Computational Methods in Applied Sciences and Engineering.

Papoutsis-Kiachagias, E.M., Porziani, S., Groth, C., Biancolini, M.E., Costa, E., Giannakoglou, K.C., 2015. Aerodynamic Optimization of Car Shapes using the Continuous Adjoint Method and an RBF Morpher. EUROGEN 2015, 11th International Conference on Evolutionary and Deterministic Methods for Design, Optimization and Control with Applications to Industrial and Societal Problems , 1–15doi:10.13140/RG.2.1.1615.2165.

Squire, W., Trapp, G., 1998. Using complex variables to estimate derivatives of real functions. SIAM Review 40, 110–112. doi:10.1137/S003614459631241X.

Thomée, V., 2001. From finite differences to finite elements. Journal of Computational and Applied Mathematics 128, 1–54. doi:10.1016/S0377-0427(00)00507-0.

Yatheendhar, M., Belegundu, A.D., 1993. Analytical shape sensitivity by implicit differentiation for general velocity fields. Computers and Structures 46, 617–623. doi:10.1016/0045-7949(93)90390-Y.